Article No. jmbi.1998.2425 available online at http://www.idealibrary.com on IDEAL J. Mol. Biol. (1999) 285, 2005–2019

JMB

Folding and Assembly of an Antibody Fv Fragment, a Heterodimer Stabilized by Antigen

Marcus Jäger and Andreas Plückthun*

Biochemisches Institut der Universität Zürich Winterthurerstr. 190 CH-8057 Zürich, Switzerland

**Corresponding author*

The folding and assembly of the Fv fragment of the phosphorylcholine binding antibody McPC603, a non-covalent heterodimer of the variable domains V_H and V_L, was investigated. Since both domains, each engineered for stability and folding efficiency, could now be obtained in native and soluble form by themselves, fluorescence spectra of V_H and V_L in unfolded, folded and associated states can be reported. V_H and V_L only associate when they are native, and the stability of the heterodimer is strongly increased in the presence of antigen. V_H rapidly folds into an hyperfluorescent intermediate, and the native state is reached in two parallel, proline-independent reactions. V_L displays two fast refolding reactions, which are followed by two slower phases, limited by proline *cis/trans*-isomerization. The rate-limiting step for both the Fv and the scFv (single-chain Fv) fragment is the formation of the native V_H-V_L interface, which depends on ProL95 being in *cis*. The folding of the Fv fragment is fast after short-term denaturation or in the presence of proline *cis/trans*-isomerase catalysis, but the scFv fragment falls into a kinetic trap, observed by the persistence of the slow phases under all conditions. Furthermore, the scFv fragment, but not the Fv fragment, gives rise to premature interface formation, indicated by the fluorescence spectra and a much higher transient binding of 8-anilino-1-naphthalene sulfonate. The analysis of the folding pathway of the domains V_H and V_L in isolation and in non-covalent and covalent assemblies should provide helpful insights into the folding of multimeric proteins in general, and for the further engineering of stable and well-folding antibody fragments in particular.

Keywords: multidomain proteins; antibody fragments; protein folding; proline *cis/trans*-isomerization; off-pathway intermediates

Introduction

In vitro refolding studies on single domain proteins have greatly contributed to our understanding of the protein folding problem (Kim & Baldwin, 1990; Matthews, 1993), and folding pathways of a number of small monomeric proteins have been elucidated to considerable molecular detail (see, for example, Udgaonkar & Baldwin, 1988; Roder *et al*., 1988; Bycroft *et al*., 1990; Radford *et al*., 1992). However, single domain proteins represent a rather limited fraction of all known proteins, as the majority of existing proteins in bacterial or animal cells has an overall molecular mass >25 kDa (Kiehn & Holland, 1970). These proteins are either composed of a single chain that folds into several domains or consist of two or more subunits, stabilized by non-covalent forces. The folding pathway of such proteins is generally complex, as it involves conformational folding of the subunits and chain association steps. These additional structural complications often lead to unproductive side reactions such as incorrect chain

Abbreviations used: ESI-MS, electrospray ionization-mass spectrometry; Fv, antibody Fv fragment, consisting of V_H and V_L; GdmCl, guanidinium hydrochloride; IMAC, immobilized metal ion affinity chromatography; NMR, nuclear magnetic resonance spectroscopy; PC, phosphorylcholine; PPIase, peptidyl-prolyl *cis/trans*-isomerase; V_H, variable domain of the antibody heavy chain; V_L, variable domain of the antibody light chain; scFv, single-chain Fv fragment; ANS, 8-anilino-1-naphthalene sulfonate; CDR, complementarity determing region.

E-mail address of the corresponding author: plueckthun@biocfebs.unizh.ch

0022-2836/99/052005–15 $30.00/0

association, and finally aggregation (Jaenicke, 1987).

Antibodies are prototypes of multidomain proteins, since they are built from well-defined building blocks, the immunoglobulin domains (Padlan, 1994). The smallest fragment of antibodies that still contains the complete antigen binding site is the Fv fragment. It is composed of the two variable domains V_L and V_H of the light and heavy chain. Both domains are of similar size (12-14 kDa), and the Fv heterodimer is stabilized by a large, hydrophobic interface. Besides their obvious direct biotechnological importance, antibody fragments have the great advantage of being a versatile model system for studying the folding behavior of multimeric proteins, since the folding of the constituting domains, their association and the folding of various covalently associated forms can be studied experimentally and compared (Goto & Hamaguchi, 1982; Tsunenaga *et al*., 1987; Lang *et al*., 1987; Lilie *et al*., 1995; Lilie, 1997; Freund *et al*., 1996, 1997a,b; Jäger & Plückthun, 1997).

The Fv fragment used here is derived from the well-characterized phosphorycholine (PC) binding antibody McPC603 (Perlmutter *et al*., 1984; Satow *et al*., 1986; Plückthun, 1993). It can be expressed in *Escherichia coli* as a functional protein and purified by hapten affinity chromatography (Skerra & Plückthun, 1988). Folding mutations were identified, which improve the *in vivo* and *in vitro* folding of the McPC603 Fv fragment (Knappik *et al*., 1995; H. Bothmann & A.P., unpublished data), and NMR backbone NH-resonances have been assigned for the Fv and scFv fragment (Freund *et al*., 1994), making this protein an interesting model system for the folding of large, multidomain proteins.

In a first series of experiments, the refolding of the McPC603 scFv fragment was characterized (Freund *et al*., 1996, 1997a,b; Jäger & Plückthun, 1997). An off-pathway kinetic trap is formed early in refolding, whose formation is favored by a high local concentration of the non-native domains V_L and V_H, caused by their covalent linkage. Here, we extend these studies to the Fv fragment (which lacks the interdomain peptide linker) and the isolated domains V_H and V_L. Using fluorescence spectroscopy, we have studied the folding of the single domains and their assembly into the heterodimer, and we have investigated the role of the interdomain linker on refolding. We exploited the fact that the constituting domains of the Fv fragment can be easily isolated in a thermodynamically stable and assembly competent state. This enabled us to compare the fluorescence emission properties of the isolated domains with those of the Fv heterodimer and to work out spectroscopic parameters, which specifically monitor heterodimerization. Next, we analyzed the kinetics of heterodimerization from the isolated native domains. This knowledge allowed us then to mix one native domain with the other undergoing a folding reaction, and finally to interpret the folding reaction obtained when both domains are allowed to fold simultaneously. The knowledge of the underlying folding pathway should serve as a basis for further detailed structural studies on these biotechnologically and biomedically important proteins.

Results

Description of the antibody fragments used

The Fv fragment described here is derived from the Fv fragment of the antibody McPC603 (Satow *et al*., 1986) and carries eight framework mutations to improve stability and folding efficiency. The V_L domain contains the stabilizing mutations A(L15)L, S(L56)P, N(L90)Q (all sequence numbering as described by Kabat *et al*., 1987). The effect on the stability on V_L of each of these mutations has been determined with stability increments of 5.7 kJ/mol (A(L15)L), 4.4 kJ/mol (N(L90)Q) and 3.0 kJ/mol (S(L56)P; Steipe *et al*., 1994; Ohage *et al*., 1997). A $(His)_5$-tag was attached to the C terminus of V_L, but not to V_H, to facilitate domain separation under native conditions (see below). The V_H domain carries the mutations P(H40)A, S(H63)A, A(H64)D, S(H79)N, I(H80)T (Jäger & Plückthun, 1997), which result in improved *in vivo* and *in vitro* folding properties (Knappik *et al*., 1995; H. Bothmann & A.P., unpublished data). If not stated explicitely, we use the term V_L wt to refer to the presence of two *cis*-proline residues (ProL8, ProL95), always in the context of these additional mutations. The second construct used, the mutant V_L P(L8)A, carries the mutation P(L8)A, also in the context of these mutations (Jäger & Plückthun, 1997). ProL8 is positioned in the outer β-sheet of the V_L domain, making no direct contact with neighboring residues. Mutagenizing ProL8 to Ala does not interfere with heterodimerization, nor with antigen binding (Jäger & Plückthun, 1997).

Spectral properties of the Fv fragment, V_H and V_L

Figure 1 shows the localization of the five tryptophan (Trp) residues in the Fv fragment. V_L contains a single tryptophan (TrpL35), which is completely buried in the hydrophobic core and in close proximity to the conserved disulfide bridge. Besides the homologous core trypthophan (Trp H36), V_H contains three additional tryptophans, either positioned within (TrpH100i) or at the edges of the CDRs (complementarity determining regions; TrpH47, TrpH103). Upon heterodimerization with V_L, these latter residues become buried in a hydrophobic interface, accompanied by a reduction of the solvent-accessible surface of the Trp side-chains from 41.7% to 0.7% (TrpH47), 47.9% to 27.6% (TrpH100i) and 35.5% to 2.3% (TrpH103).

To monitor the folding of the Fv fragment spectroscopically, we first recorded fluorescence emission spectra of the heterodimer and the two isolated domains in the native and completely

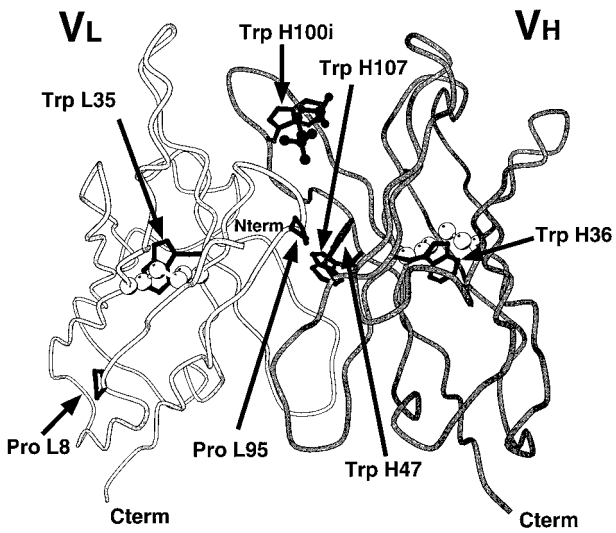

Figure 1. Location of the tryptophan residues of the Fv fragment of the phosphorylcholine binding antibody McPC603. Quarternary structure of the Fv heterodimer, composed of V_L (grey) and V_H (dark grey). The five tryptophan residues and the two *cis*-proline residues are highlighted, with the side-chains shown in grey and black, respectively. The single disulfide bond in V_L and V_H is represented in ball-and-stick form. The antigen phosphorylcholine is also included in ball-and-stick representation.

denatured state (4 M guanidinium hydrochloride (GdmCl)). The fluorescence of native V_L is strongly quenched, and unfolding is characterized by a fluorescence increase (Figure 2(a)). Similar observations have been made for other V_L domains, and this effect has been interpreted as a dequenching of the fluorescence of the conserved core-Trp by the disulfide bond upon unfolding (Goto & Hamaguchi, 1979, 1982; Tsunenaga *et al.*, 1987; Frisch *et al.*, 1996). Due to the higher Trp-content, V_H shows a much higher intrinsic fluorescence than V_L. The emission maximum of the native protein (346 nm) indicates that the Trp residues are mainly solvent exposed (see above). Unfolding of V_H results in a large fluorescence increase at 370 nm, but only a minimal red-shift in the emission spectrum is detectable (to 348 nm).

When the emission spectrum of the native Fv fragment is compared with the arithmetic sum of the emission spectra of native V_H and V_L at a 1:1 stoichiometric ratio, a blue-shift in the emission maximum from 346 nm to 331 nm can be noticed upon going from the single domains to the ''real'' Fv fragment, with a maximal relative fluorescence increase at 328 nm (Figure 2(b)). This optical change must be due to heterodimerization of V_L and V_H, and can be rationalized by a change in the environment of TrpH47, TrpH100i and TrpH103 upon interface formation (Figure 1). The antigen alone, the small hapten phosphorylcholine (PC), does not show any intrinsic fluorescence, nor does its binding to the Fv fragment change the intrinsic

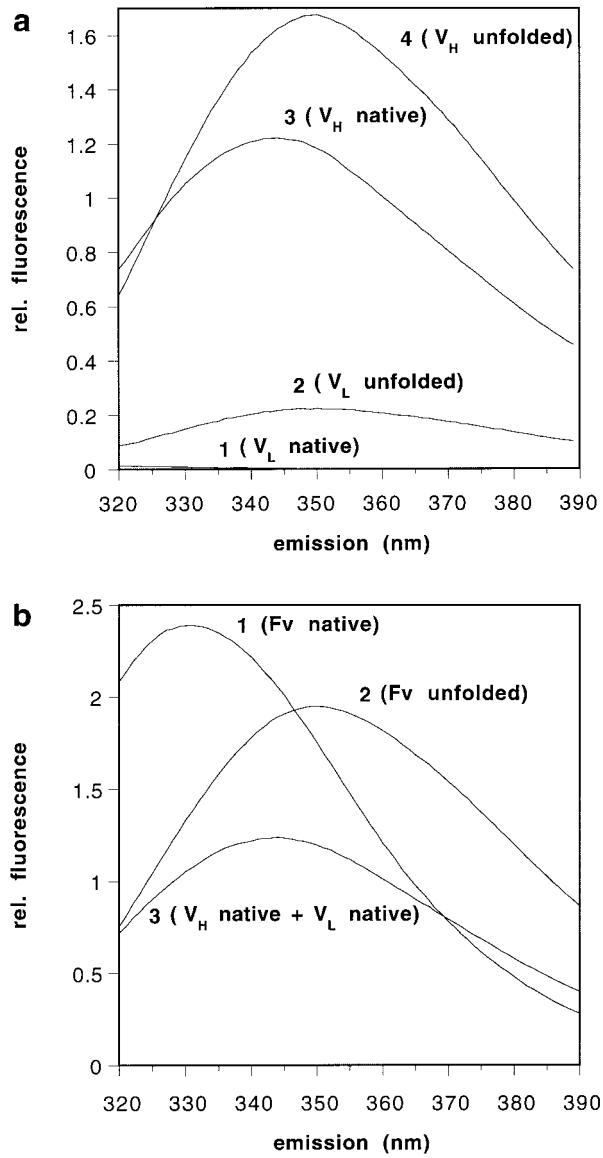

Figure 2. Static fluorescence emission spectra of the Fv fragment and the isolated domains. (a) Native (spectrum 1) and unfolded V_L (spectrum 2), native (spectrum 3) and unfolded V_H (spectrum 4). (b) Native Fv fragment (spectrum 1), computational addition of native V_L and native V_H (1:1 stoichometry; spectrum 3) and unfolded Fv fragment (spectrum 2). Spectra were recorded in buffer E and all fluorescence intensities in (a) and (b) were normalized to the fluorescence of native V_H at 328 nm, which was set to 1.0. Thus, the scale in (a) and (b) is directly comparable. The protein concentration was 1.0 μM, except for spectrum 1 of (a), which was 4.0 μM.

protein fluorescence when excited at 295 nm. Antigen binding only becomes observable upon excitation at 280 nm by a 10% increase in protein fluorescence (Glockshuber *et al.*, 1990), presumably because the antigen makes direct contact with TyrL100 of the V_L domain (Satow *et al.*, 1986). The emission spectrum of the unfolded Fv fragment (emission maximum = 349 nm) is comparable with

the algebraic sum of spectra of denatured V_H and V_L, consistent with complete chain dissociation (Figure 2(b)). Taken together, these data show that the domain heterodimerization in the Fv fragment can be almost selectively monitored by a large fluorescence increase at 328 nm.

Thermodynamic stability of V_H and V_L

GdmCl titrations of V_L were carried out by recording the fluorescence at 350 nm (the maximum of the difference spectrum of native and fully unfolded V_L). Fluorescence was excited at 280 nm.

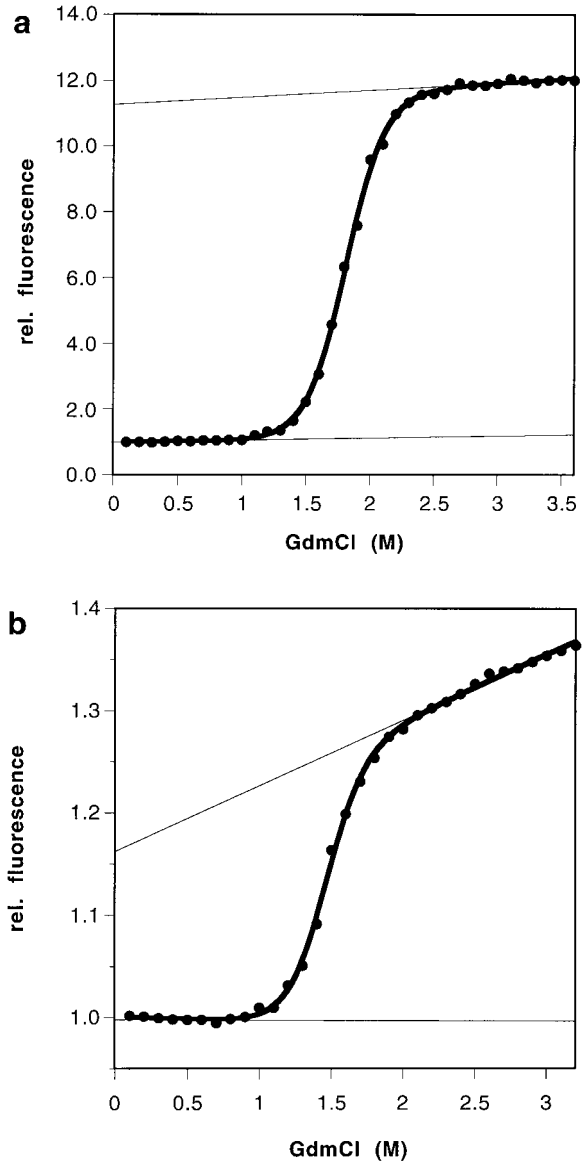

Figure 3. Thermodynamic stability of V_L and V_H. (a) Equilibrium unfolding of the V_L domain. (b) Equilibrium unfolding of the V_H domain. Measurements were carried out by recording the change in fluorescence emission intensity at 350 nm (a) or 370 nm (b). Protein concentrations were 0.5 μM. The straight lines show the fluorescence dependence of the native and unfolded baselines.

Figure 3(a) shows a cooperative unfolding transition between 1.0 and 2.3 M GdmCl, with a midpoint of unfolding at approximately 1.7 M GdmCl. There is only a modest dependence of the fluorescence emission intensity on [GdmCl] in the pre and post-unfolding region of the equilibrium unfolding transition. The equilibrium free energy difference $\Delta G_{N\text{-}U}$ between native and unfolded V_L is 27.9 kJ/mol, and a cooperativity value m_G of 15.4 kJ mol^{-1} M^{-1} was determined. This result shows that the increase in stability achieved by the simultaneous introduction of all three mutations into V_L (14.2 kJ/mol) corresponds very well with the computational addition of the stability increments determined for the single mutations (13.1 kJ/mol; Steipe *et al.*, 1994; Ohage *et al.*, 1997; see above).

The equilibrium unfolding of V_H was investigated by monitoring the change in fluorescence intensity at 370 nm (the maximum of the difference spectrum of native and fully unfolded V_H; Figure 3(b)). Unfolding of V_H is cooperative between 0.8 and 2.0 M GdmCl, and shows a midpoint of unfolding at about 1.4 M GdmCl. However, pre and post-unfolding baselines are steeper in V_H than in V_L. The calculated equilibrium free energy difference $\Delta G_{N\text{-}U}$ between native and unfolded V_H (27.1 kJ/mol) is comparable with that of V_L (28.5 kJ/mol), but the unfolding transition seems to be slightly more cooperative ($m_G = 18.7$ kJ mol^{-1} M^{-1}). In contrast to V_L, we cannot make any statement about the effect of the five framework mutations in V_H on stability, since the wt V_H domain tends to aggregate (Knappik *et al.*, 1996; Glockshuber *et al.*, 1992). Nevertheless, all five mutations introduced simultaneously into the V_H domain largely increase the yield of the Fv fragment and almost completely abolish the formation of aggregates *in vivo* (H. Bothmann, unpublished data).

Reconstitution of the Fv fragment from native V_L and V_H

Native V_H was titrated with native V_L in the presence of 5 mM antigen (Figure 4(a)). A plot of the fluorescence increase at 328 nm *versus* the V_L/V_H ratio is linear up to the equivalence point at stoichiometric domain concentrations, but then sharply levels off after increasing the concentration of V_L beyond that of V_H (Figure 4(b), filled circles). The spectral properties of the protein solution at the stoichometric equivalence point were identical with those of affinity-purified Fv fragment (Figure 2). The maximal fluorescence increase at equimolar domain concentrations is consistent with a tight and quantitative assembly of the heterodimer from V_H and V_L, provided that antigen is included in the buffer to stabilize the Fv heterodimer. In the absence of antigen, the heterodimer is less stable. The fluorescence increase at 328 nm was hyperbolic rather than linear in the absence of antigen (Figure 4(b), open circles), and

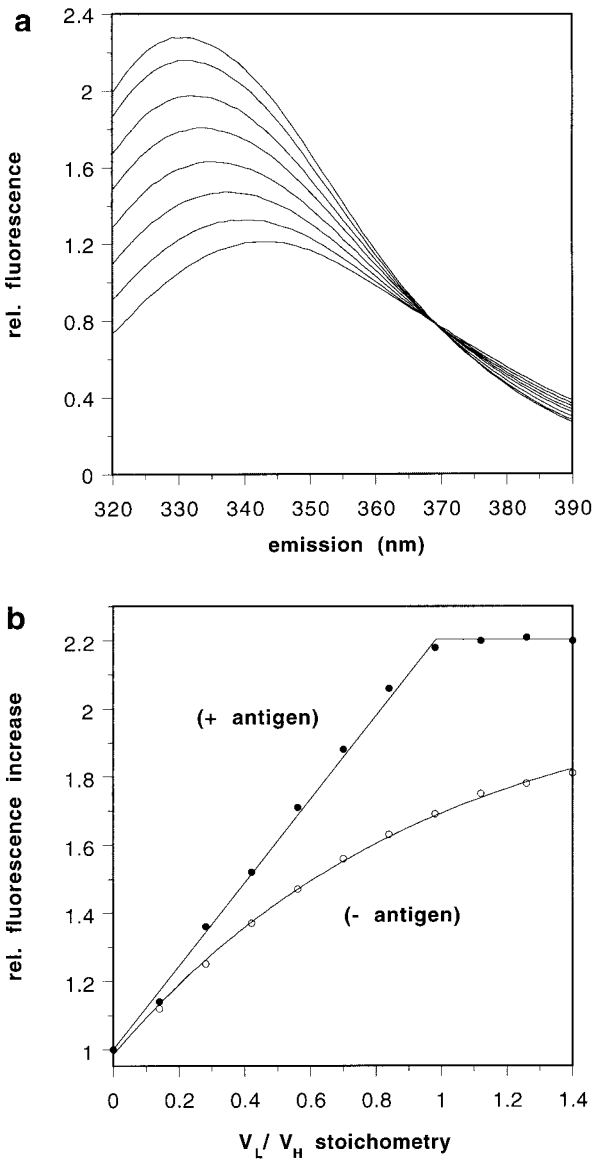

Figure 4. Reconstitution of the Fv fragment from native domains. (a) Native V_H (0.7 μM, spectrum 1) was titrated with native V_L (35 μM stock solution) in buffer E. The fluorescence is normalized to the fluorescence of native V_H at 328 nm (lowest spectrum), which was set to 1.0. (b) Plot of the fluorescence at 328 nm obtained after the addition of native V_L to native V_H *versus* the V_L/V_H ratio. Filled circles, in the presence of antigen (buffer E; open circles, in the absence of antigen (buffer D).

at the stoichometric equivalence point at 0.7 μM, only 65% of the chains are assembled into the Fv heterodimer. The data can be fit to a dissociation constant of 2×10^{-7} M for the dissociation of the Fv fragment into V_H and V_L, if V_L dimerization is considered negligible. Simulations indicate that the data can only be accomodated with dissociation constants for the V_L dimer of micromolar or weaker, and thus the influence of an V_L dimerization on the calculated dissociation constant of the Fv fragment must indeed be very small (data not shown).

Kinetics of assembly of the Fv heterodimer from native domains

Since V_H and V_L represent thermodynamically stable entities (Figure 3) that remain fully association-competent in isolated form (Figure 4), domain assembly can be decoupled from domain folding. This allows us to study the domain association reaction of V_H and V_L into the Fv heterodimer in detail. Heterodimerization rates were measured by mixing V_H with an equal volume of V_L in the presence of 5 mM antigen, and the net fluorescence increase occurring at > 305 nm was monitored as a function of time. The antigen was included in the refolding buffer to achieve quantitative chain assembly, and thus maximal fluorescence amplitudes (Figure 4(b)). To establish pseudo-first order conditions, the concentration of V_H was kept constant, while the concentration of V_L was in excess and varied. As the contribution of native V_L to the measured fluorescence is minimal (Figure 2), the measured amplitude is directly proportional to the extent of heterodimerization. The fluorescence increase was monoexponential, and identical fluorescence amplitudes were obtained at all V_L concentrations used (Figure 5(a); for reasons of clarity, only three out of five fluorescence traces are shown). A plot of the apparent rate constant (k_{obs}) is linear in $[V_L]$, indicating that the bimolecular chain association is rate limiting under these conditions and that no conformational change is kinetically relevant for domain association (Figure 5(b)). The slope of such a plot is the bimolecular association rate constant (k_{on}), where $k_{obs} = k_{on} \cdot [V_L] + k_{off}$. The value of the slope is 1.2×10^5 s^{-1} M^{-1} at 10 °C. The dissociation rate constant of the Fv heteromer (k_{off}) is given by the intercept of the slope, which was close to zero under the experimental conditions, as the backreaction was prevented by antigen.

Refolding kinetics of the isolated V_H domain

In agreement with the equilibrium unfolding transition (Figure 3(b)), refolding of the isolated V_H domain (1 μM) gave only a small fluorescence decrease at 370 nm (data not shown). However, there was an unexpectedly large fluorescence decrease at 328 nm (ca. 30% compared with the intrinsic fluorescence of native V_H) upon folding (Figure 6(a), trace 1), while the equilibrium unfolding transition predicted only a very modest fluorescence decrease (<10%) at this wavelength (data not shown). The fluorescence trace at 328 nm could be fit to a biexponential function ($k_{fast} = 0.065$ s^{-1}; rel. amplitude$_{fast} = 0.85$; $k_{slow} = 0.012$ s^{-1}, rel. amplitude$_{slow} = 0.15$). Identical kinetics were obtained for short-term (ten seconds unfolding in 4 M GdmCl) and long-term unfolded V_H (>24 hour unfolding in 4 M GdmCl), as well as at lower protein concentration (0.5 μM; data not shown). We therefore interpret the biphasic refolding kinetics of V_H in terms of two

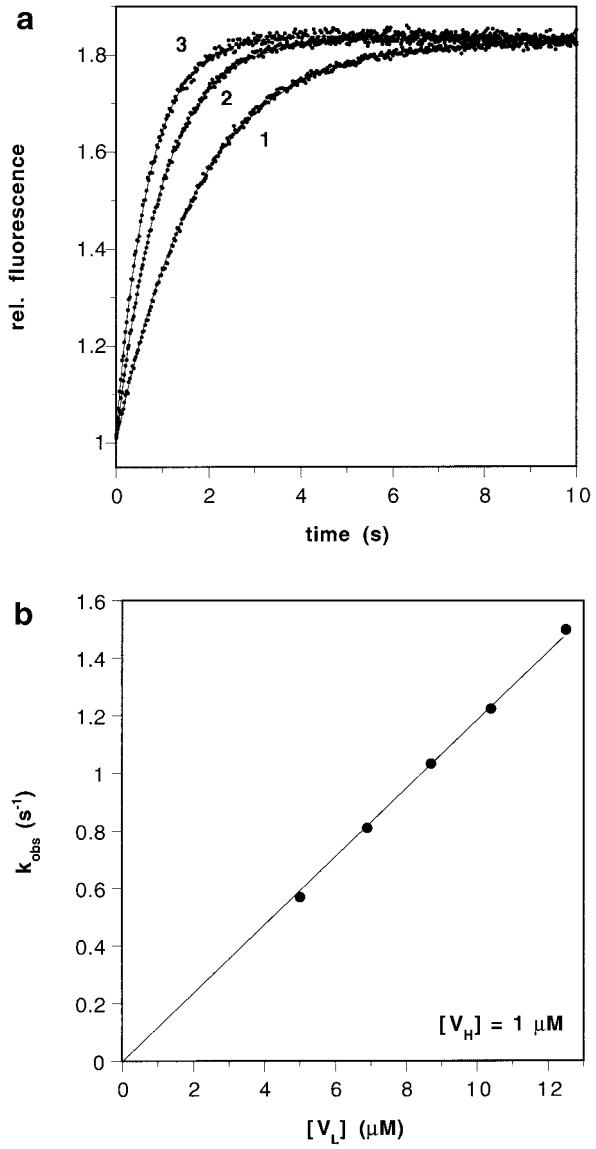

Figure 5. Kinetics of assembly of the Fv fragment from native domains. (a) Native V_H (2 μM) was mixed 1:1 with native V_L in buffer E and the fluorescence change at >305 nm was recorded. Shown are kinetic traces obtained after mixing V_H with 10 μM V_L (final concentration) (trace 1), 17.4 μM V_L (trace 2) and 25 μM V_L (trace 3). The fluorescence obtained after mixing native V_H with buffer containing no V_L was set to 1.0. (b) Plot of the apparent rate constant k_{obs} *versus* $[V_L]$.

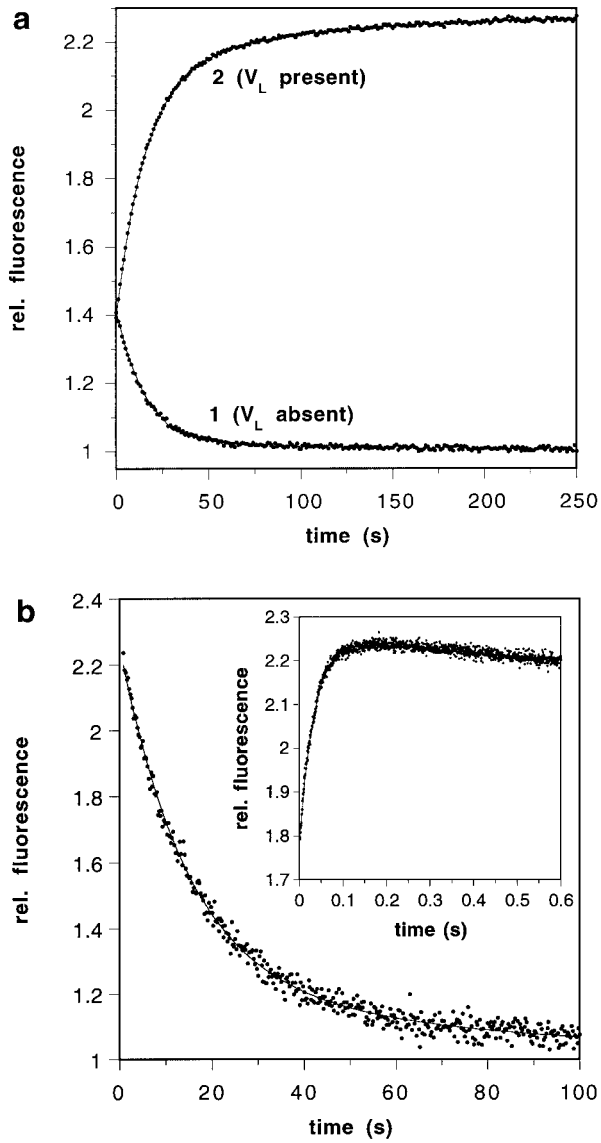

Figure 6. Refolding kinetics of the V_H domain. (a) Unfolded V_H (100 μM, in 4 M GdmCl) was manually diluted 1:100 into buffer E in the absence (trace 1) and presence of 4.0 μM native V_L (trace 2). The fluorescence is normalized to the fluorescence of native V_H at 328 nm, which was arbitrarily set to 1.0. (b) Unfolded V_H (50 μM, in 4 M GdmCl) was diluted 1:25 into buffer E in a stopped-flow apparatus. The fluorescence at >305 nm was recorded after excitation at 295 nm. The insert shows an enlarged view of the first 0.6 seconds, with the fast fluorescence increase and the onset of the slow fluorescence decrease, measured in a separate kinetic experiment at higher time-resolution. In both experiments, the fluorescence is normalized to the fluorescence at infinite time obtained after fitting (b), which was arbitrarily set to 1.0.

intramolecular steps, both of which are apparently independent of proline *cis/trans*-isomerization. This conclusion is reasonable as the V_H domain contains no *cis*-proline residues and only a single *trans*-proline (ProH44), which is positioned in a solvent-exposed loop (Satow *et al.*, 1986).

Since the equilibrium unfolding (Figure 3(b)) predicted a much smaller fluorescence decrease at 328 nm upon folding than was observed, we reasoned that there must have been a rapid increase in fluorescence undetectable in the manual mixing experiments. To resolve this fluorescence increase at 328 nm kinetically, we performed stopped-flow experiments (Figure 6(b)). There is indeed a rapid, monophasic fluorescence increase ($k = 31\ s^{-1}$), followed by a much slower fluorescence decrease ($k = 0.056\ s^{-1}$). Despite small differences in the refolding conditions (manual

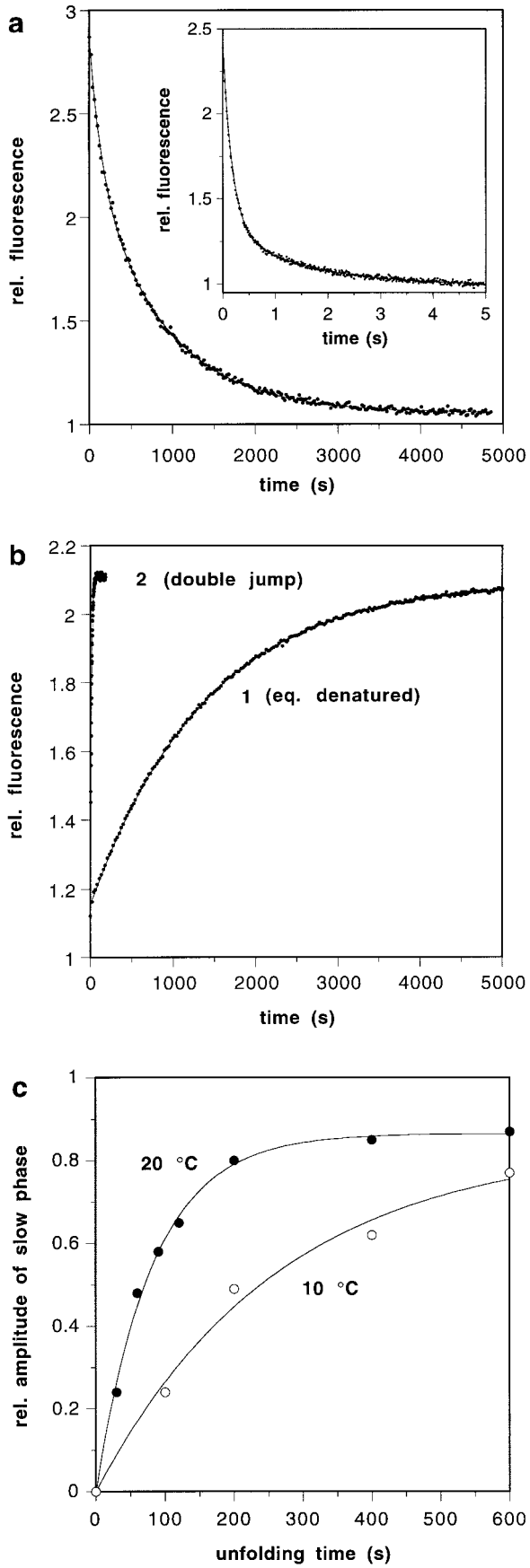

Figure 7. Refolding kinetics of the V_L domain. (a) Unfolded V_L (250 μM, in 4 M GdmCl) was diluted 1:100 into buffer E. Fluorescence emission was normalized to the intrinsic fluorescence of native V_L at 350 nm, which was set to 1.0. The inset shows a representative stopped-flow refolding trace obtained after a 1:25 dilution of long-term denatured V_L (50 μM, in 4 M GdmCl) into buffer E. (b) Long-term (trace 1) and short-term (trace 2) denatured V_L (100 μM, in 6 M GdmCl) was diluted 1:100 into buffer E containing 1.10 μM native V_H. Fluorescence emission is normalized to the fluorescence of a mixture of native V_H and V_L at a 1:1 stoichometry at 328 nm, which was set to 1.0. (c) Plot of the relative fraction of the slow folding amplitude *versus* the unfolding time. Filled circles, unfolding at 20 °C; open circles, unfolding at 10 °C.

refolding: 0.04 M GdmCl, stopped-flow refolding: 0.16 M GdmCl), the rate of the fluorescence decrease in the stopped-flow experiment is in reasonable agreement with the faster of the two manually resolvable phases ($k = 0.064\ s^{-1}$). The slower of the two manually resolvable phases could not be resolved in the stopped-flow experiment, as photobleaching and diffusion artefacts only allowed data aquisition <100 seconds.

Refolding kinetics of the V_H domain in the presence of native V_L

In order to gain further insight into the complex kinetics, V_H (1 μM) was also refolded in the presence of a large stoichometric excess of native V_L (4 μM) and 5 mM antigen, and the fluorescence increase at 328 nm was recorded (Figure 6(a), trace 2). In this experiment, refolding of V_H is monitored indirectly by the fluorescence increase that occurs upon heterodimerization with V_L (Figure 2(b)). The initial fluorescence intensity in the presence of V_L was identical with that of V_H alone (native V_L being almost invisible; Figure 2(a)), but a biphasic fluorescence increase was observable thereafter. Relative amplitudes and kinetic rate constants of both phases were similar to those obtained in the absence of V_L ($k_{fast} = 0.06\ s^{-1}$, rel. amplitude$_{fast} = 0.82$; $k_{slow} = 0.012\ s^{-1}$, rel. amplitude$_{slow} = 0.18$). Identical rate constants were obtained at higher V_L concentration (10 μM; data not shown), indicating that folding of V_H is completely rate-limiting in the presence of high stoichometric excess of native V_L over V_H. Also, the observed rates were much smaller than the heterodimerization rates expected for V_H and V_L at the concentrations used (Figure 5).

Refolding of the isolated V_L domain

Refolding of V_L (2.5 μM) was followed by monitoring the fluorescence at 350 nm (Figure 7(a)). A biphasic fluorescence decrease was obtained after manual mixing ($k_{fast} = 0.009\ s^{-1}$, rel. amplitude$_{fast} = 0.30$; $k_{slow} = 0.00085\ s^{-1}$, rel. amplitude$_{slow} = 0.70$). However, the two manual phases accounted for only about 25 % of the fluor-

escence amplitude expected from the equilibrium unfolding transition, corrected for pre and post-transition fluorescence baseline dependencies (Figure 3(a)). This indicates that a significant fraction of the fluorescence amplitude escaped detection in the manual mixing experiment. Efforts to slow down the refolding reaction using higher GdmCl concentrations and thus to increase the manually resolvable fluorescence amplitude were unsuccessful. Even at 0.8 M GdmCl, still about 75 % of the calculated fluorescence amplitude was lost in the dead-time of manual mixing. The rates of the two manually resolvable phases decreased only slightly from 0.0072 s^{-1} at 0.04 M GdmCl to 0.005 s^{-1} at 0.8 M GdmCl (fast manual phase) and from 0.00085 s^{-1} at 0.04 M GdmCl to 0.00078 s^{-1} at 0.8 M GdmCl (slow manual phase). As > 90 % of the manually resolvable fluorescence amplitude disappeared after short-term unfolding, we believe that both slow phases are limited by proline *cis/trans*-isomerization (data not shown).

To kinetically resolve the fluorescence decrease lost in the dead-time of manual mixing, we also performed stopped-flow experiments with V_L. Two phases, both showing a fluorescence decrease, were detectable ($k_{fast} = 10\ s^{-1}$; rel. amplitude$_{fast} = 0.90$; $k_{slow} = 0.50\ s^{-1}$; rel. amplitude$_{slow} = 0.10$; Figure 7(a), inset). Because the stopped-flow reaction is measured with a cut-off filter, we cannot quantitatively add the amplitudes of the manual and stopped-flow phases. Consequently, we cannot completely rule out the existence of yet another phase occuring in the dead-time of the stopped-flow experiment. As most of the fluorescence decrease is occuring in the dead-time of manual mixing (cf. Figure 3(a) and Figure 7(a)), the quenching of the principal chromophor TrpL35 must have largely occured after few seconds of refolding, indicating that it must be juxtaposed to the disulfide bond at this time.

Folding of V_L is rate-limiting for the assembly of the Fv fragment

In a third experiment, we refolded long-term denatured V_L (1.0 μM) in the presence of native V_H (1.1 (M) and 5 mM antigen. As shown above for the reciprocal experiment, the folding of V_H in the presence of native V_L (Figure 6(a)), such an assay measures heterodimer assembly, observable by the large fluorescence increase at 328 nm (Figure 2(b)). The fluorescence emission at 328 nm upon addition of denatured V_L was only slightly higher than the fluorescence of native V_H before the addition of V_L (time 0 in Figure 7(b), trace 1), ruling out significant interface formation in the dead-time of manual mixing. The fluorescence was gained in a very slow, monoexponential reaction, and the rate constant of this slow increase (0.00073 s^{-1}) was in good agreement with the slowest observable phase of V_L (0.00085 s^{-1}; Figure 7(a)). Mixing of short-term unfolded V_L with native V_H leads to significantly faster assembly of the Fv heterodimer, and the whole fluorescence amplitude is gained in a monoexponential reaction with a rate constant of 0.10 s^{-1}. This corresponds with a roughly 100-fold acceleration when compared with the rate of the same reaction performed with equilibrium-unfolded V_L. As significant differences in the refolding rate of long and short-term unfolded proteins are typical for proline-limited reactions (Reimer *et al.*, 1998), we suggest that *cis/trans*-isomerization around critical proline-peptide bonds in V_L is rate-limiting for the formation of the Fv heterodimer. This effect can be quantitatively examined by measuring the relative amplitude of the slow phase, which becomes larger upon increasing the time between unfolding and refolding (Figure 7(c)), as an isomerization from *cis* to *trans* proline residues occurs in the denatured state, with rates and temperature dependence typical for these reactions (Grathwohl & Wüthrich, 1981; Adler & Scheraga, 1990).

The results described here for the Fv fragment indicate a different behavior than for the scFv fragment (Freund *et al.*, 1997a,b; Jäger & Plückthun, 1997). Using H/D-NMR and fluorescence spectroscopy, it could be shown that short-term denatured scFv refolds in two parallel pathways into the native state. However, the fraction of the scFv folding *via* the fast track does not exceed 30-35 %, while the remainder takes a slow folding pathway, with a rate constant typical for long-term denatured scFv. The large fraction of slowly folding species in the scFv fragment, which is furthermore increased by the addition of PPIase (peptidyl-proly *cis/trans*-isomerase), led us to propose the existence of a off-pathway kinetic trap, formed rapidly after initiation of refolding (Freund *et al.*, 1997a,b; Jäger & Plückthun, 1997). In contrast, the data described here indicate that no such a trap exists for the assembly of the Fv fragment from an unfolded V_L domain and a native V_H domain. It thus seems that the trap is only formed if both domains are present in non-native conformation and at high local concentration (provided by the interdomain peptide linker in the scFv).

Cis/trans-isomerization at ProL95 precedes heterodimerization and is a prerequisite for the assembly of the Fv-fragment

The assembly of the Fv fragment is rate-limited by proline *cis/trans*-isomerization. The high relative amplitude (>0.90) of the slow association phase on the total fluorescence increase is evidence that at least one of the two *cis*-proline residues (ProL8, ProL95; Satow *et al.*, 1986) contributes to the rate-limiting step. *Cis*-ProL8 is positioned in the outer β-sheet of the V_L domain, making no direct contact with the rest of the domain (Figure 1). Earlier studies showed that ProL8 can be replaced by Ala without interfering with heterodimerization and antigen binding (Jäger & Plückthun, 1997). Therefore, long-term denatured V_L P(L8)A was refolded

in the presence of native V_H, while monitoring heterodimer formation as described above (Figure 7(b)). Interestingly, the P(L8)A mutation did not influence the rate of chain assembly ($k_{slow} = 0.00078\ s^{-1}$), and very similar relative amplitudes were found for the slow fluorescence increase (Figure 8(a), trace 1). Since faster chain association was observed in the presence of PPIase (Figure 8(a), trace 2 and 3; Figure 8(b)), we conclude that *cis/trans*-isomerization at ProL95 is rate-limiting for the assembly of the Fv fragment. A direct proof of this hypothesis is, however, not possible. Due to the key role of ProL95 in mediating the V_H-V_L interaction (Figure 1; Satow *et al.*, 1986), removal of ProL95 destabilizes the Fv heterodimer and results in chain dissociation.

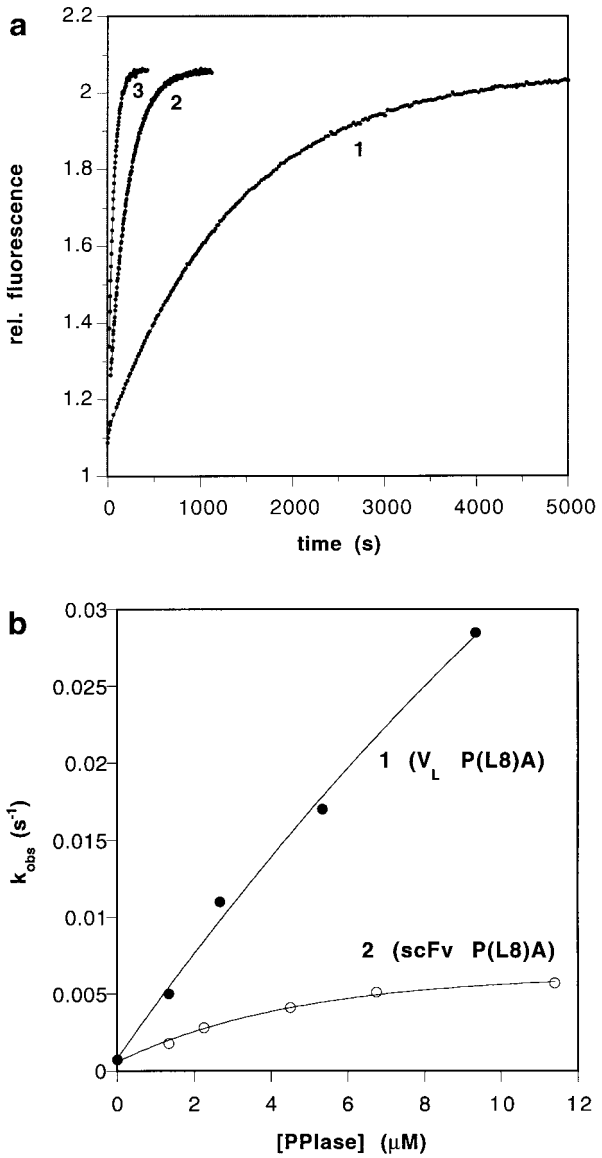

Figure 8. The role of *cis*-ProL8 on the assembly of the Fv fragment. (a) Unfolded V_L P(L8)A (100 μM, in 4 M GdmCl) was diluted 1:100 into buffer E containing 1.10 μM native V_H and the change in fluorescence emission at 328 nm was recorded. Long-term unfolded V_L P(L8)A in the absence of PPIase (trace 1), in the presence of 2.66 μM PPIase (trace 2) and 9.33 μM PPIase (trace 3). The fluorescence was normalized to the fluorescence of a mixture of native V_H and V_L at a 1:1 stoichometry at 328 nm, which was set to 1.0. (b) Plot of the observed association rate constant *versus* [PPIase] in the refolding buffer for long-term unfolded V_L P(L8)A in the presence of native V_H.

Whereas the folding rate of V_L P(L8)A increased almost linearly with PPIase in the range of 0-10 μM (Figure 8(b)), catalysis of the corresponding scFv P(L8)A is less effective and reaches a plateau within the same concentration range of enzyme (Freund *et al.*, 1997a,b; Jäger & Plückthun, 1997). In principle, the differences in catalysis might be thought to arise from a reduced accessibility of one or more critical prolyl-peptide bonds in the scFv, relative to those in the V_L domain. However, if this were the only difference, identical fast refolding behavior after short-term unfolding (with native prolyl-peptide bonds exclusively) would be expected for the Fv and scFv fragment, which is clearly not the case (see Freund *et al.*, 1997a,b; Jäger & Plückthun, 1997). Thus, it seems plausible that the plateau-level reported for the scFv directly monitors the return from the off-pathway trap in the folding of the scFv fragment, in the presence of maximal PPIase catalysis.

Kinetics of assembly of the Fv fragment from unfolded V_H and V_L and comparison with refolding of the scFv fragment

The refolding trace (emission at 328 nm) of long-term denatured Fv fragment at a 1:1 chain-stoichometry is shown in Figure 9(a). The rate constant for the slow fluorescence increase ($0.00062\ s^{-1}$) is comparable with the rate obtained for refolding of V_L in the presence of native V_H ($0.00078\ s^{-1}$; Figure 7(a)), which was ProL95-limited. This slow phase is preceeded by a fast fluorescence decrease, which is not observable during refolding of V_L in the presence of native V_H (Figure 9(a), inset). As the rate constant of this fast fluorescence decrease ($0.082\ s^{-1}$) was similar to the rate constant of the fast folding phase of V_H ($0.065\ s^{-1}$; Figure 6(a), trace 1), we assign this early phase of the Fv fragment to the folding of V_H.

While the refolding of the scFv fragment, monitored by Trp-fluorescence spectroscopy, shows a qualitatively similar refolding behavior (Figure 9(b); fast fluorescence decrease, slow fluorescence increase), there are some noteworthy differences. First, the earliest measurable fluorescence emission after manual mixing is much higher in intensity (compare initial fluorescence intensities in Figures 9(a) and 10(a)). Second, the fast fluorescence decrease, which in the Fv fragment was assigned mainly to the folding of the V_H domain, seems to be reduced in amplitude and smaller in rate ($0.02\ s^{-1}$) in the scFv fragment (compare insets in Figure 9(a) and (b)). Therefore, the relative amplitude of the slow fluorescence increase is also

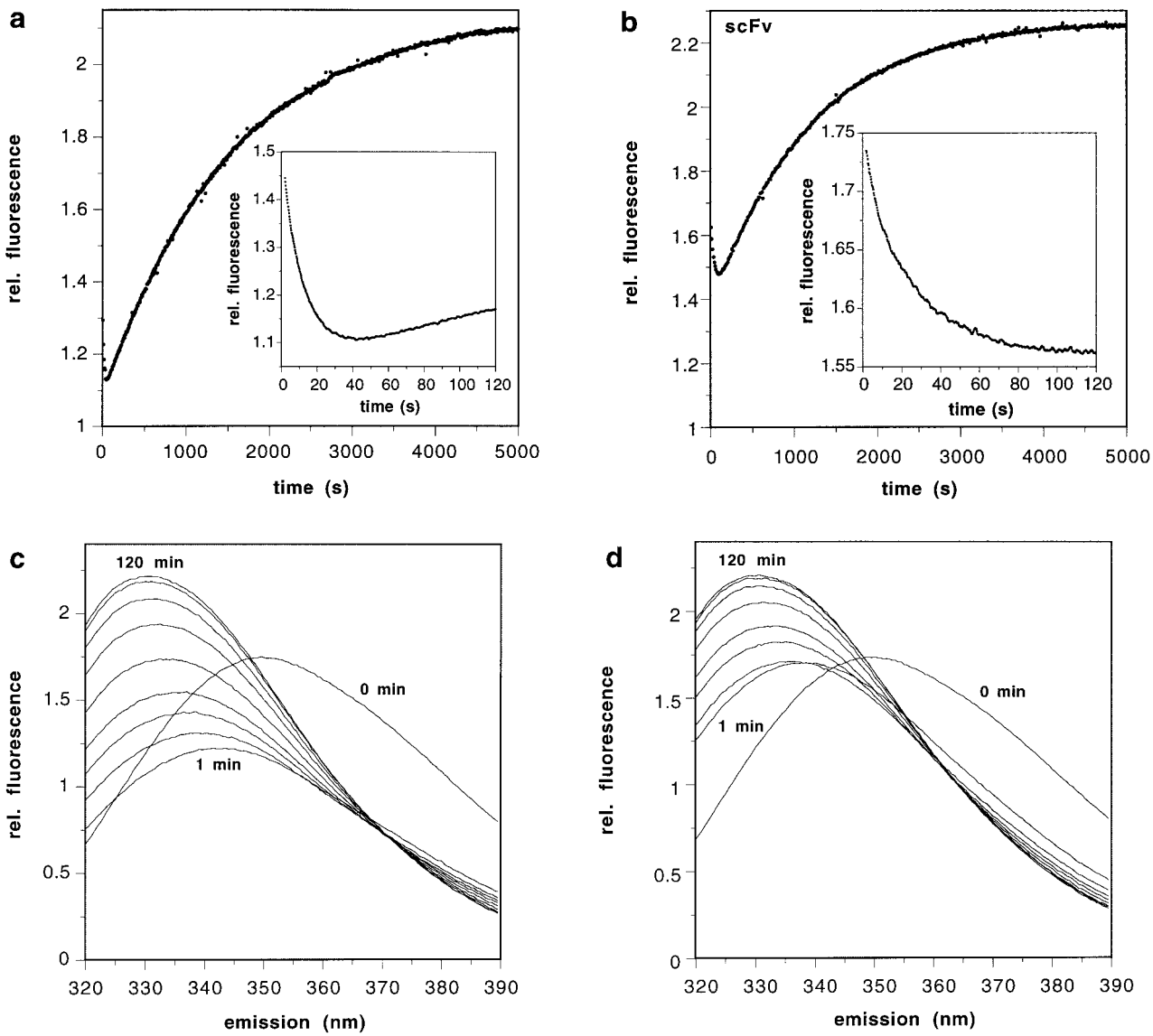

Figure 9. Refolding kinetics of the Fv and scFv fragment. (a) Long-term denatured Fv fragment (100 μM, in 4 M GdmCl) was diluted 1:100 into buffer E and the fluorescence at 328 nm was recorded. The fluorescence was normalized to the fluorescence of a mixture of native V_H and V_L at a 1:1 stoichometry at 328 nm, which was set to 1.0. The insert shows an enlarged view of the early kinetics, measured separately at higher time-resolution under otherwise identical conditions. (b) Refolding of long-term denatured scFv performed as described in (a). (c) Refolding of the Fv fragment monitored by recording fluorescence emission spectra after 1 minute, 5 minutes, 10 minutes, 25 minutes, 40 minutes, 60 minutes, 90 minutes and 120 minutes. The emission spectrum of the fully denatured protein is also shown (labeled 0 minutes). (d) Refolding of the scFv fragment monitored by recording fluorescence emission spectra after 1 minute, 5 minutes, 10 minutes, 25 minutes, 40 minutes, 60 minutes, 90 minutes and 120 minutes.

smaller in the scFv fragment, even though the kinetic rate constant of this phase (0.00087 s^{-1}) seems to be not significantly affected by the linker peptide. The increased initial fluorescence in the scFv supports our view of an early domain interaction. This quarternary interaction is, however, premature and does not result from faster folding of the scFv. Earlier H/D-quench-flow and NMR-studies on wt McPC603 showed that native scFv is formed in a slow reaction, with a kinetics comparable to the slow fluorescence increase described here (Freund *et al.*, 1996, 1997b).

These conclusions are supported by an inspection of the whole fluorescence spectra, which can be conveniently recorded during the refolding reaction, since this is very slow. In the case of the Fv fragment, the earliest recordable time point (one minute) is very similar to an algebraic sum of native V_H and native V_L (Figure 2(a)), where native V_H dominates the spectrum. In contrast, in the spectrum of the scFv fragment the earliest recordable time point (one minute) shows a blue-shifted emission maximum and a higher fluorescence intensity at 328 nm, suggesting a hydrophobic

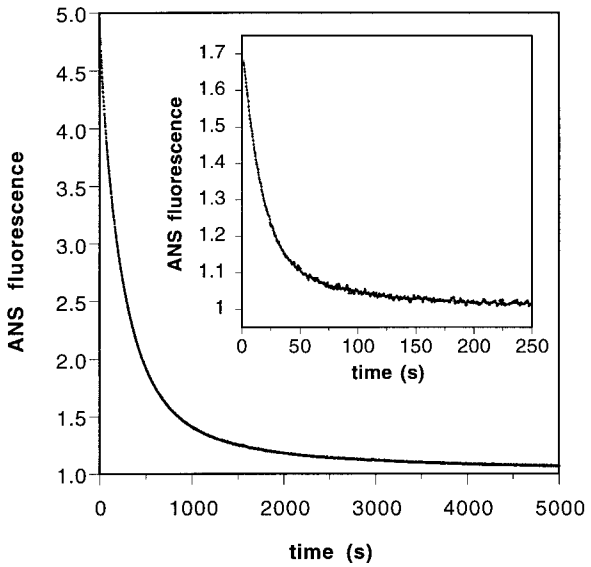

Figure 10. Refolding kinetics of the Fv and scFv fragment in the presence of the fluorescent dye ANS. Refolding of short-term denatured scFv fragment and Fv fragment (inset) in the presence of 50 μM ANS. Excitation was at 370 nm and dye fluorescence was monitored at 480 nm. Protein concentration was 0.5 μM. Fluorescence intensities are normalized to the ANS fluorescence in the absence of protein and were set to 1.0.

environment of the interface tryptophan residues and thus some kind of interface formation.

Folding of the Fv and scFv fragment monitored by the extrinsic fluorescence dye ANS

ANS (8-anilino-1-naphthalene-sulfonate) is a fluorescence dye, which shows only little intrinsic fluorescence in polar solvents, but strongly increased fluorescence in apolar solvents (Haugland, 1991). No or only little (<5 %) increase in ANS fluorescence is seen in the presence of unfolded (4 M GdmCl) or native scFv fragment, respectively (data not shown). If short-term denatured scFv is refolded in the presence of ANS, however, significantly increased dye fluorescence is detectable (Figure 10), indicating strong binding of ANS to one or more refolding intermediates of the scFv within the deadtime of manual mixing (five seconds). Increased ANS fluorescence has been observed for a number of proteins (Ptitsyn *et al.*, 1990) in non-native states, and this observation has been attributed to the formation of molten globule-type states, with a more mobile packing and solvent-accessible hydrophobic patches, favoring dye binding. ANS desorption, indicating increased core packing, proceeds in a biphasic reaction ($k_{fast} = 0.004\ s^{-1}$, rel. amplitude$_{fast} = 0.75$; $k_{slow} = 0.0011\ s^{-1}$, rel. amplitude$_{slow} = 0.25$).

We also carried out the ANS experiment with the Fv fragment under identical conditions (Figure 10, inset). To our surprise, the manually resolvable fluorescence amplitude was significantly reduced, and desorption was also significantly faster, albeit still biphasic. Interestingly, there was excellent agreement between the rates and relative amplitudes of ANS desorption of the Fv fragment (rate$_{fast} = 0.060\ s^{-1}$, rel. amplitude$_{fast} = 0.83$; rate$_{slow} = 0.012\ s^{-1}$; rel. amplitude$_{slow} = 0.17$) and the refolding rates of the isolated V_H domain, monitored by the change in the intrinsic Trp-fluorescence ($k_{fast} = 0.065\ s^{-1}$; rel. amplitude$_{fast} = 0.85\ s^{-1}$; $k_{slow} = 0.012\ s^{-1}$; rel. amplitude$_{slow} = 0.15$; Figure 6(a), trace 1). Control experiments with the isolated V_L domain showed no detectable ANS binding, while experiments with the isolated V_H domain showed dye binding and desorption identical to the Fv fragment.

Taken together, these data show that covalent coupling of V_L and V_H into a scFv fragment favors the population of an intermediate, not detectable in the refolding of the Fv fragment, nor in V_H or V_L. This molten globule-type intermediate seems to be only partially folded, with a significant kinetic barrier separating this state from the native state.

Discussion

We have investigated the folding and assembly of the Fv fragment of an antibody, by first measuring the association of the native chains, then the folding of the individual domains, and finally domain folding and assembly simultaneously. We chose the Fv fragment of the antibody McPC603 as a model system. After engineering V_L and V_H for stability and lack of aggregation, both domains can now be obtained in association-competent form. They can form quantitatively the V_L-V_H heterodimer upon mixing, and the equilibrium can be conveniently and rapidly shifted by the small hapten phosphorylcholine, whose binding is furthermore spectroscopically silent. Thus, quantitative domain association can be observed, even though their mutual affinity is low enough in the absence of antigen to exist partially as single domains at low protein concentration. Low chain affinity in the absence of antigen was also described for other Fv fragments (Riechmann *et al.*, 1988; King *et al.*, 1993). A large fluorescence increase occurs upon the formation of the McPC603 heterodimer from the isolated domains, and this can be used to study the folding of the isolated V_L and V_H , as well as their assembly into the Fv fragment independently. Domain association is monophasic, and a second-order association rate constant of $1.2 \times 10^5\ M^{-1}\ s^{-1}$ was determined at 10 °C. This value is typical for protein-protein interaction at moderate ionic strength (Vijayakumar *et al.*, 1998) and is consistent with measurements of the association of the light and heavy chain of antibody F_{ab} fragments (Friedman *et al.*, 1978; Watt & Voss, 1979) and antibody-antigen interactions (Ward *et al.*, 1989).

Refolding of the V_H domain

Refolding of V_H is fast when compared with long-term denatured V_L. First, a hyperfluorescent intermediate is formed within 200 ms after initiation of refolding, followed by a much slower, biphasic fluorescence decrease. In the presence of native V_L, V_H can assemble with V_L into the Fv heterodimer as soon as V_H is native. At high stoichometric excess of native V_L over V_H, the refolding of V_H becomes rate-limiting, and a biphasic fluorescence increase is observed. From a kinetic point of view, both the direct (V_H alone) and the indirect folding experiment (V_H in the presence of native V_L) give rise to identical kinetic parameters. Due to the lack of kinetic data on isolated antibody V_H domains, a mechanistic interpretation for McPC603 V_H is difficult at this point. From the current data, we suggest two parallel-folding-pathways for V_H. Parallel folding would directly explain why identical refolding kinetics of V_H are observed in the presence and absence of V_L, yet with fluorescence amplitudes of opposite sign. If the reactions were sequential, V_L should dock either after the first or the second phase of V_H, and only one of the phases should be visible as interface formation. Clearly, more detailed studies are needed to corrobate this view and to get a better understanding of the observed intermediates in structural terms.

Refolding of the V_L domain

V_L contains seven proline residues (two *cis*-proline residues, five *trans*-proline residues), while V_H contains only a single *trans*-proline. Refolding of V_L is multiphasic and, in contrast to V_H, slowed down by proline *cis/trans*-isomerization. Two stopped-flow phases are detectable for long-term denatured V_L. Both phases show a fluorescence decrease, which suggests that the core-TrpL35 becomes located next to the disulfide bond and quenched within the first seconds of refolding. While a biphasic fluorescence decrease with similar kinetic rate constants and relative amplitudes is also found for the V_L domain of the humanized antibody 4D5 (Carter *et al*., 1992; M.J., unpublished data), we have no further insight into the biphasic nature of this process so far. The two stopped-flow phases are followed by two significantly slower phases, also detectable by a fluorescence decrease and resolvable by manual mixing. Both of these slow phases dissapear after short-term unfolding, indicating that both phases might be related to proline *cis/trans*-isomerization. The small relative amplitude of the manually resolvable phases on the total folding amplitude (about 25 %) indicates that a conformation with largely native-like fluorescence properties is already adopted before the start of these phases with non-native prolyl-peptide bonds. This view is also supported by recent H/D-exchange studies on the scFv wt fragment of the antibody McPC603 (Freund *et al*., 1996, 1997a). While the protein used in that study did not contain any of the mutations discussed here, a weakly exchange-resistant intermediate in the inner β-sheet of the V_L domain of the scFv fragment was detected, formed in the dead-time of the quench-flow experiment (10 ms; Freund *et al*., 1996, 1997a), indicating at least some formation of structure in V_L in this short time. However, more structural work is clearly necessary to interpret the fluorescence data of V_L in structural terms.

Proline *cis/trans*-isomerization is rate-limiting for the assembly of the Fv fragment after mixing long-term denatured V_L with native V_H. A *cis*-ProL95 is necessary for the formation of stable Fv heterodimers, giving rise to a major fraction (>90 %) of slowly associating V_L after long-term unfolding. PPIase accelerates the assembly of the Fv fragment from long-term denatured V_L and native V_H by catalyzing the *cis/trans*-isomerization at the critical ProL95. Fast chain assembly is also observed in the absence of PPIase for short-term denatured V_L with native prolyl-peptidyl bonds. The importance of the *cis*-ProL95 for the formation of stable heterodimers can be rationalized from the crystal structure of the McPC603 F_{ab} fragment (Satow *et al*., 1986; Jäger & Plückthun, 1997). ProL95, located at the edge of CDR 3, correctly positions AspL91, TyrL94 and LeuL96, all of which are involved in salt-bridges and hydrogen bonds with residues of the V_H domain. A *trans*-ProL95 might disturb these interactions and destabilize the heterodimer, even in the presence of excess of antigen, which was shown to stabilize the heterodimer against chain dissociation, but which may not bind in the distorted binding site.

Refolding of the Fv heterodimer and the influence of the linker peptide in the scFv fragment

If stoichometric amounts of long-term denatured V_H and V_L are refolded together, both domains start to refold independently of each other. V_L first converts to a compact intermediate with ProL95 mostly in *trans*. As a consequence, refolding of V_H is seen by a fluorescence decrease, as the formation of stable heterodimers is impeded with a *trans*-ProL95 in V_L. After the very slow formation of the *cis*-ProL95 V_L in the rate-limiting step of the refolding reaction, both domains assemble into the Fv heterodimer in a monoexponential reaction, and this reaction can be followed by a fluorescence increase upon interface formation.

While the global folding behavior of the Fv fragment is similar to the scFv fragment, refolding of the latter is characterized by the existence of a kinetic trap, an intermediate in which V_L and V_H prematurely associate, before *cis/trans*-isomerization at ProL95 permits correct and stable association to the native interface. While the formation and the return from the trap are not rate-limiting for refolding of long-term scFv fragment, the trap does compete with the fast folding of short-term

denatured protein into the native state (Freund *et al*., 1997b; Jäger & Plückthun, 1997). There is no evidence for such a kinetic trap during refolding of the V_L domain in the presence of native V_H (Figure 7(a)), as short-term denatured V_L assembles with V_H into the Fv fragment in a monoexponential reaction. It appears, therefore, that the trap only forms in significant amounts when both V_L and V_H, in non-native form, are forced close together by a linker, suggesting that they do not have a high degree of affinity for each other. A similar effect was described by Tsunenaga *et al*. (1987) for a whole antibody light chain. Refolding of the light chain was clearly different from the sum of the single domains V_L and C_L, with an additional very slow phase observed only in the whole light chain. With the NMR resonance assignment available for the McPC603 Fv and scFv fragment (Freund *et al*., 1994), a detailed study of the refolding pathway of the Fv fragment and V_H and V_L on the one side, and the scFv fragment on the other side, by quench-flow H/D exchange in combination with NMR and ESI-MS (electrospray ionization-mass spectroscopy), should provide residue-specific insights into the nature of the kinetic trap of the scFv fragment. The kinetic framework presented here should be helpful in designing suitable experiments.

Materials and Methods

Materials

Phosphorylcholine (calcium salt) was from Sigma, GdmCl (molecular biology grade) was from Fluka and used without further purification.

Protein expression and purification

The Fv fragment was expressed at 25 °C in the *E. coli* K12 strain JM83 (Vieira & Messing, 1982) and secreted into the periplasm to allow disulfide formation. Cells were grown in LB broth at ambient temperature, and protein expression was induced with IPTG (1 mM final concentration) at an A_{550} of 1.0. Cells were harvested after five hours induction by centrifugation and periplasmic extracts were prepared as described (Lindner *et al*., 1992). All subsequent chromatographic steps were performed at 4 °C. Functional Fv fragment was purified from periplasmic extracts on a PC-Sepharose affinity column, equilibrated in buffer A (50 mM sodium borate, 400 mM NaCl (pH 7.6)). After washing with buffer A, the Fv fragment was eluted with buffer B (50 mM sodium borate, 400 mM NaCl, 5 mM PC (pH 7.6)). For further purification to homogeneity, the Fv fragment was concentrated (Centricon 10) to approximately 3 mg/ml and chromatographed at 0.8 ml/per minute on a gel filtration column (Sephacryl S100, HiPrep 26/60; Pharmacia), equilibrated in buffer B. The Fv fragment eluted in a symmetrical peak at the expected molecular weight (25-27 kDa) and peak fractions were collected. For the isolation of native V_H and V_L, the purified Fv fragment was exhaustively dialyzed against buffer A to remove the antigen, whose binding stabilizes the heterodimer (see below), and applied at 1 ml per minute onto an IMAC column (Ni-trinitriloacetate, Qiagen), equilibrated in the same buffer. After collection of V_H in the flow-through, the column was washed extensively with buffer A. V_L was eluted with buffer C (50 mM sodium borate; 400 mM NaCl, 100 mM imidazole (pH 7.6)). Typically, yields of >90 % were achieved for both domains. Rotamase (PpiA), a periplasmic *E. coli* peptidyl-prolyl-*cis*/*trans* isomerase (PPIase), was purified as described (Liu & Walsh, 1990). PPIase activity was checked according to standard assay protocols (Fischer *et al*., 1984). Protein purity was ascertained by non-reducing SDS-15 % PAGE, and the integrity of the protein preparations was confirmed by ESI-MS (data not shown). Protein concentrations were determined using absorption coefficients calculated as described by Gill & von Hippel (1989).

Fluorescence spectroscopy

Steady-state and kinetic fluorescence experiments were performed at 10 °C with a PTI Alpha Scan spectrofluorimeter (Photon Technologies, Inc.) under gentle magnetic stirring. Slid widths of 1.5 and 8 nm were used for excitation and emission, respectively.

Equilibrium denaturation experiments

Protein/GdmCl-mixtures (2 ml) containing a final protein concentration of 0.5 μM and denaturant concentrations ranging from 0 to 4 M GdmCl were prepared from freshly purified protein (in buffer D) and a GdmCl stock solution (8 M, in 20 mM Mes (pH 5.7)). After overnight incubation at 10 °C, the fluorescence emission intensity of each sample was recorded at 350 nm (V_L) or 370 nm (V_H). Excitation was at 280 nm (V_L) or 295 nm (V_H). Fluorescence intensities at the given wavelength were plotted *versus* the GdmCl concentration. Protein stabilities were calculated from these plots by nonlinear least-squares fitting of the following equation (Pace, 1990):

$$F_{(D)} = \{(F_N + m_N[D]) + (F_U + m_U[D]) \exp[-(\Delta G_{N-U} + m_G[D])/RT]\}/[1 + \exp[-(\Delta G_{N-U} + m_G[D])/RT]\}$$

where $F_{(D)}$ is the value of the specified optical parameter (fluorescence emission intensity at 350 nm or 328 nm) at denaturant concentration $[D]$; F_N and F_U represent the calculated values of F linearily extrapolated to $[D] = 0$ for the native and unfolded protein, respectively; m_N and m_U are the slopes of the pre and post-unfolding baselines, respectively; $\Delta G_{N\text{-}U}$ is the free energy difference for unfolding in the absence of denaturant; m_G represents the slope of the free energy change *versus* denaturant concentration, assuming a linear relationship between the free energy of unfolding, ΔG_{obs}, and $[D]$; R is the gas constant; and T is the absolute temperature.

Domain titration experiments

Native V_H in buffer D (20 mM Mes (pH 5.7)) or buffer E (20 mM Mes (pH 5.7), 5 mM PC; see text for details) were titrated with a solution of native V_L in buffer D. After equilibration for 15 minutes, emission spectra were recorded from 320 nm to 390 nm after excitation at 295 nm and corrected for background fluorescence and dilution, which was minimal.

Manual refolding experiments

Manual refolding experiments were performed by following the fluorescence emission intensity at a fixed wavelength after excitation at either 280 nm or 295 nm (see Figure legends and text for details). Two different types of manual refolding experiments are described in the text. In the first type of experiments, native protein was denatured in 4 M GdmCl (final concentration, in buffer E) and allowed to equilibrate for at least 24 hours at 10 °C to enable all prolyl-peptide bonds to reach equilibrium (equilibrium/long-term denatured protein). Refolding was then started by manual dilution of denatured protein into buffer E. In the second type of experiments, native protein was only briefly denatured in 6 M GdmCl for ten seconds on ice before the refolding reaction was initiated (double jump/short-term denatured protein). Stopped-flow experiments indicated complete unfolding in less than five seconds under these conditions (Freund *et al*., 1997b; M.J. & A.P., unpublished results). The brief unfolding time guarantees that all prolyl-peptide bonds retain their native conformation (Brandts *et al*., 1975). Data of fast reactions (< ten minutes) were recorded in the open shutter mode. For slow reactions (> ten minutes), the fluorescence intensity was measured at preset intervals, while keeping the shutter closed between measurements to prevent photobleaching. Fluorescence traces were evaluated using the program Kaleidagraph (Synergy software, Reading).

Stopped-flow fluorimetry

Stopped-flow fluorescence experiments were performed at 10 °C with an Applied Photophysics model SX-17MV spectrofluorimeter. Domain association rates were measured by a 1:1 (v:v) mixing of native V_H with a stoichometric excess of native V_L in buffer E (see the text for details), and the overall change in fluorescence emission intensity at >305 nm was integrated by the use of a cut-off filter (excitation at 295 nm). The refolding kinetics of V_H and V_L was initiated by a 1:25 (v:v) mixing of unfolded protein (50 μM in 4 M GdmCl) into buffer E, and the change in protein fluorescence emission intensity at >305 nm was integrated using a cut-off filter (excitation at 295 nm). Typically, four to eight fluorescence traces were averaged, smoothed with the software provided by Applied Photophysics and fit to a sum of exponentials using the program Kaleidagraph.

ANS desorption experiments

Refolding experiments in the presence of the dye 8-anilino-1-naphthalene-sulfonate (ANS) contained 50 μM ANS and 0.5 μM protein in buffer E. Excitation was at 370 nm and dye fluorescence was recorded at 480 nm. The concentration of ANS was determined in methanol, using an extinction coefficient of 6800 M^{-1} cm^{-1} at 370 nm (Haugland, 1991).

Acknowledgments

We would like to thank Dr Annemarie Honegger for help in the preparation of Figure 1 and to Prof. John Robinson, Organisch-chemisches Institut, for access to his stopped-flow apparatus. This work was supported by the Schweizerische Nationalfonds, grant 3100-046624.96/1.

References

Adler, M. & Scheraga, H. A. (1990). Non-native isomers of proline 93 and 114 predominate in heat-unfolded ribonuclease A. *Biochemistry,* **29**, 8211-8219.

Brandts, J. F., Halvorson, H. R. & Brennan, M. (1975). Consideration of the possibility that the slow step in protein denaturation reactions is due to *cis-trans* isomerism of proline residues. *Biochemistry,* **14**, 4953-4960.

Bycroft, M., Matouschek, A., Kellis, J. T., Jr, Serrano, L. & Fersht, A. R. (1990). Detection and characterization of a folding intermediate in barnase by NMR. *Nature,* **346**, 488-490.

Carter, P., Presta, L., Gorman, C. M., Ridgway, J. B. B., Henner, D., Wong, W.-L., Rowland, A. M., Kotts, C. E., Carver, M. E. & Shephard, H. M. (1992). Humanization of an anti-$p185^{HER2}$ antibody for human cancer therapy. *Proc. Natl Acad. Sci. USA,* **89**, 4285-4289.

Fischer, G., Bang, H., Berger, E. & Schellenberger, A. (1984). Conformational specificity of chymotrypsin toward proline-containing substrates. *Biomed. Biophys. Acta,* **791**, 87-97.

Freund, C., Ross, A., Plückthun, A. & Holak, T. A. (1994). Structural and dynamic properties of the Fv fragment and the scFv fragment of an antibody in solution investigated by heteronuclear three-dimensional NMR spectroscopy. *Biochemistry,* **33**, 3296-3303.

Freund, C., Honegger, A., Hunziker, P., Holak, T. A. & Plückthun, A. (1996). Folding nuclei of the scFv fragment of an antibody. *Biochemistry*, **35**, 8457-8464.

Freund, C., Gehrig, P., Holak, T. A. & Plückthun, A. (1997a). Comparison of the H/D exchange behavior of the rapidly formed folding intermediate and the native state of the scFv fragment of an antibody. *FEBS Letters,* **407**, 42-46.

Freund, C., Gehrig, P., Baici, A., Holak, T. A. & Plückthun, A. (1997b). Parallel pathways in the folding of a short-term denatured scFv fragment of an antibody. *Fold. Design*, **3**, 39-49.

Friedman, F. K., Chang, M. Y. & Beychok, S. (1978). Kinetics of interaction of heavy and light chains in immunoglobulins. *J. Biol. Chem.* **7**, 2368-2372.

Frisch, C., Kolmar, H., Schmidt, A., Kleemann, G., Reinhardt, A., Pohl, E., Uson, I., Schneider, T. R. & Fritz, H. J. (1996). Contribution of the intramolecular disulfide bridge to the folding stability of REIv, the variable domain of a human immunoglobulin kappa light chain. *Fold. Design,* **1**, 431-440.

Gill, S. C. & von Hippel, P. H. (1989). Calculation of protein absorption coefficients from amino acid sequence data. *Anal. Biochem.* **182**, 319-326.

Glockshuber, R., Malia, M., Pfitzinger, I. & Plückthun, A. (1990). A comparison of strategies to stabilize immunoglobulin Fv fragments. *Biochemistry,* **29**, 1362-1367.

Goto, Y. & Hamaguchi, K. (1979). The role of the intrachain disulfide bond in the conformation and stability of the constant fragment of the immunoglobulin light chain. *J. Biochem.* **86**, 1433-1441.

Goto, Y. & Hamaguchi, K. (1982). Unfolding and refolding of the constant fragment of the immunoglobulin light chain. *J. Mol. Biol,* **156**, 891-910.

Grathwohl, C. & Wüthrich, K. (1981). NMR studies of the rates of proline *cis/trans*-isomerization in oligopeptides. *Biopolymers,* **20**, 2623-2633.

Haugland, R. P. (1991). *Handbook of Fluorescent Probes and Research Chemicals*, Molecular Probes, Inc., Eugene, OR.

Jaenicke, R. (1987). Folding and association of proteins. *Prog. Biophys. Mol. Biol.* **49**, 117-237.

Jäger, M. & Plückthun, A. (1997). The rate-limiting steps for the folding of an antibody scFv fragment. *FEBS Letters,* **418**, 106-110.

Kabat, E. A., Wu, T. T., Reid-Miller, M., Perry, H. M. & Gottesmann, K. (1987). *Sequences of proteins of immunological interest*, Public Health Science, National Institues of Health, Bethesda, USA, Maryland.

Kiehn, E. D. & Holland, J. J. (1970). Size distribution of polypeptide chains in cells. *Nature,* **226**, 544-545.

Kim, P. & Baldwin, R. L. (1990). Intermediates in the folding reactions of small proteins. *Annu. Rev. Biochem,* **59**, 631-660.

King, D. J., Byron, O. D., Mountain, A., Weir, N., Harvey, A., Lawson, A. D. G., Proudfoot, K. A., Baldock, D. A. & Owens, J. R. (1993). Expression, purification and characterization of B72.3 Fv fragments. *Biochem. J.* **290**, 723-729.

Knappik, A. & Plückthun, A. (1995). Engineered turns of a recombinant antibody improve its *in vivo* folding. *Protein Eng.* **8**, 81-89.

Koide, S., Dyson, J. H. & Wright, P. E. (1993). Characterization of a folding intermediate of apoplastocyanin trapped by proline isomerization. *Biochemistry,* **32**, 12299-12310.

Lang, K., Fischer, G. & Schmid, F. X. (1987). Catalysis of protein folding by prolyl isomerase. *Nature,* **329**, 268-270.

Lilie, H. (1997). Folding of the Fab fragment within the intact antibody. *FEBS Letters,* **417**, 239-242.

Lilie, H., Rudolph, R. & Buchner, J. (1995). Association of antibody chains at different stages of folding: Prolyl isomerization occurs after formation of quaternary structure. *J. Mol. Biol.* **248**, 190-201.

Lindner, P., Guth, B., Wülfing, C., Krebber, C., Steipe, B., Müller, F. & Plückthun, A. (1992). Purification of native proteins from the cytoplasm and periplasm of *Escherichia coli* using IMAC and histidine tails: a comparison of proteins and protocols. *Methods: A Companion to Methods in Enzymology,* **4**, 41-56.

Liu, J. & Walsh, C. T. (1990). Peptidyl-prolyl *cis-trans*-isomerase from *Escherichia coli* a periplasmic homolog of cyclophilin that is not inhibited by cyclosporin A. *Proc. Natl Acad. Sci. USA,* **87**, 4028-4032.

Matthews, C. R. (1993). Pathways of protein folding. *Annu. Rev. Biochem.* **62**, 653-683.

Ohage, E. A., Graml, W., Walter, M. M., Steinbacher, S. & Steipe, B. (1997). β-turn propensities as paradigms for the analysis of structural motifs to engineer protein stability. *Protein Sci.* **6**, 233-241.

Pace, C. N. (1990). Measuring and increasing protein stability. *Trends Biotechnol.* **8**, 93-98.

Padlan, E. A. (1994). Anatomy of the antibody molecule. *Mol. Immunol.* **31**, 169-217.

Perlmutter, R. M., Crews, S. T., Douglas, R., Sorensen, G., Johnson, N., Nivera, N., Gerhart, P. J. & Hood, L. (1984). The generation of diversity in phosphorylcholin-binding antibodies. *Advan. Immunol.* **25**, 1-37.

Plückthun, A. (1992). Mono- and bivalent antibody fragments produced in *Escherichia coli* engineering, folding and antigen binding. *Immunol. Rev.* **130**, 151-188.

Ptitsyn, O. B., Pain, R. H., Semisotnow, G. V., Zerovnik, E. & Razgulyaev, O. I. (1990). Evidence for a molten globule state as a general intermediate in protein folding. *FEBS Letters,* **262**, 20-26.

Radford, S. E., Dobson, C. M. & Evans, P. A. (1992). The folding of hen lysozyme involves partially structured intermediates and multiple pathways. *Nature,* **358**, 302-307.

Reimer, U., Scherer, G., Drewello, M., Kruber, S., Schutkowski, M. & Fischer, G. (1998). Side-chain effects on peptidyl-prolyl *cis/trans*-isomerization. *J. Mol. Biol.* **279**, 449-460.

Riechmann, L., Foote, J. & Winter, G. (1989). Expression of an antibody Fv fragment in myeloma cells. *J. Mol. Biol.* **203,**, 825-828.

Roder, H., Elöve, G. & Englander, S. W. (1988). Structural characterization of folding intermediates in cytochrome c by H-exchange labelling and proton NMR. *Nature,* **335**, 700-704.

Satow, Y., Cohen, G. H., Padlan, E. A. & Davies, D. R. (1986). Phosphorylcholine binding immunoglobulin Fab McPC603. *J. Mol. Biol.* **190**, 593-604.

Skerra, A. & Plückthun, A. (1988). Assembly of a functional Fv fragment in *Escherichia coli*. *Science,* **240**, 1038-1041.

Steipe, B., Schiller, B., Plückthun, A. & Steinbacher, S. (1994). Sequence statistics reliably predict stabilizing mutations in a protein domain. *J. Mol. Biol.* **240**, 188-192.

Tsunenaga, M., Goto, Y., Kawata, Y. & Hamaguchi, K. (1987). Unfolding and refolding of a immunoglobulin light chain and its variable and constant fragment. *Biochemistry,* **26**, 6044-6051.

Udgaonkar, J. B. & Baldwin, R. L. (1988). NMR evidence for an early framework intermediate on the folding pathway of ribonuclease A. *Nature,* **335**, 694-699.

Vijayakumar, M., Wong, K.-Y., Schreiber, G., Fersht, A. R., Szabo, A. & Zhou, H.-X. (1998). Electrostatic enhancement of diffusion-controlled protein-protein association: comparison of theory and experiment on barnase and barstar. *J. Mol. Biol.* **278**, 1015-1024.

Vieira, J. & Messing, J. (1982). The pUC plasmids, an M13mp7–derived system for insertion mutagenesis and sequencing with synthetic universal primers. *Gene,* **19**, 259-268.

Ward, E. S., Güssow, D., Griffith, A. D., Jones, P. T. & Winter, G. (1989). Binding activities of a repertoire of single immunoglobulin variable domains secreted from *Escherichia coli*. *Nature,* **341**, 544-546.

Watt, R. M. & Voss, E. W. (1979). Recombination of heavy and light chains of immunoglobulins. *J. Biol. Chem.* **15**, 7105-7110.

Edited by P. E. Wright

(Received 18 September 1998; received in revised form 16 November 1998; accepted 17 November 1998)